Int. J. Electrochem. Sci., 15 **(2020)** 11058 – 11069, doi: 10.20964/2020.11.64

International Journal of
ELECTROCHEMICAL
SCIENCE
www.electrochemsci.org

Multi-walled Carbon Nanotubes-Modified Glassy Carbon Electrode for the Detection of Anthracene

Fredrick M. Mwazighe

TU Chemnitz, Faculty of Natural Sciences, Institute of Chemistry, AG Elektrochemie, Strasse der Nationen, 09111 Chemnitz, Germany
E-mail: fmwazighe@gmail.com

Received: 11 June 2020 / *Accepted:* 17 September 2020 / *Published:* 30 September 2020

The electrochemical oxidation of anthracene on a bare glassy carbon electrode results in electrode fouling and reduced sensitivity in its detection. Multi-walled carbon nanotubes were used to modify a glassy carbon electrode for the electrochemical detection of anthracene because of their antifouling and peak enhancement properties. The peak current for anthracene oxidation was enhanced by 73.64%, and the peak potential shifted by 53 mV to a slightly less positive value. The electrochemical process was determined to be mixed diffusion- and adsorption-controlled, and a preconcentration or accumulation time was necessary in the analysis of anthracene. Square wave voltammetry was used to analyze increasing concentrations of anthracene; a dynamic linear range of 50–146 µM (R^2 = 0.98452) and a limit of detection of 42 µM were established. The sensor platform was used to detect anthracene in a spiked sample of tap water, albeit at lower than expected concentrations because of its low solubility in water.

Keywords: anthracene, electrochemical detection, multi-walled carbon nanotubes, glassy carbon electrode.

1. INTRODUCTION

Anthracene belongs to a group of organic compounds referred to as polycyclic aromatic hydrocarbons (PAHs) [1, 2]. These compounds result from the incomplete combustion of organic materials in processes such as fuel combustion, forest fires and burning of tobacco in cigarette smoking [3, 4]. PAHs tend to adsorb on particulate matter, become transported over long distances and end up in environmental matrices such as water, soil and sediment [5]. Because they are ubiquitous in the environment, they may end up in food and water for human consumption. These compounds are important environmental pollutants because some have been shown to be carcinogenic and mutagenic from animal studies and require monitoring. Although anthracene is not identified as such, its common

occurrence in environmental samples has informed the decision by environmental organizations such as US EPA to list it as a priority compound for monitoring [2, 6, 7].

Electrochemical detection of anthracene offers a cheap, fast, and simple alternative to the conventional methods like gas chromatography and high-performance liquid chromatography. However, the conventional methods are still the most sensitive [8-10]. Efforts to improve the sensitivity of the electrochemical method involved the use of metallic and metal oxide nanoparticles, conducting polymers, and graphene to modify a working electrode [11-13]. Nanomaterials are used to impart electrocatalytic properties to the platform, and the conducting polymers provide an anchor for the nanomaterials on the electrode and inhibit electrode fouling. Although improved sensitivity has been noted in the modified electrodes, some of them have a high background current, which makes it impossible to distinguish different PAHs.

Multi-walled carbon nanotubes (MWCNTs) used in the electrochemical detection of various analytes have shown improved sensitivity, reduction of overpotentials, and inhibition of surface fouling of the working electrode while maintaining the distinctiveness of the analyte signal [14, 15]. Boikanyo used MWCNTs with metal oxide nanoparticles to modify an electrode to detect pyrene reporting improved sensitivity [16]. This process has not been attempted for other PAHs; thus, in this work, the electrochemical detection of anthracene on a glassy carbon electrode modified with MWCNTs was explored.

2. MATERIALS AND METHODS

2.1. Chemicals

All chemicals were used as received without further purification. Pure water obtained from Seralpur Pro 90CN was used. Acetonitrile (HPLC-grade 99.95% VWR International S.A.S, Fontenay-sous-Bois, France), anthracene (99.9% from Sigma Aldrich), lithium perchlorate $LiClO_4$ (> 98% Sigma Aldrich Chemie GmbH, Steinheim), alumina slurries of sizes 1.0, 0.3, and 0.05 µm (Buehler, Lake Bluff, Il, USA), multi-walled carbon nanotubes (O. D × L 6-9 nm ×5 µm, >95% C, Sigma Aldrich Chemie GmbH, Steinheim), dimethylformamide DMF (VEB Jenapharm Laborchemie Apolda), potassium ferricyanide $K_3Fe(CN)_6$ (>99%, VEB Kali-Chemie, Berlin, Germany), potassium ferrocynide $K_4Fe(CN)_6{\cdot}3H_2O$ (>99%, VEB Kali-Chemie, Berlin, Germany), and potassium chloride KCl (>99% Acros Organics, New Jersey, USA) were used.

2.2. Apparatus

Electrochemical measurements were conducted in a three-electrode system composed of a platinum plate electrode, a mercury/mercurous sulphate electrode (Hg/Hg_2SO_4, 0.1 M K_2SO_4), and a glassy carbon electrode (GCE, 0.073 cm^2) as the counter, reference and working electrodes, respectively. A H-electrochemical cell was used for preliminary experiments and a single-chamber cell (50 mL) was used for the variable concentration experiments. Cyclic voltammetry experiments were conducted using

a PG 310 potentiostat (HEKA Elektronik Dr. Schulze GmbH, Lambrecht, Germany), while square wave voltammetric measurements were performed using Ivium Stat Electrochemical Interface (EK Technologies GmbH, Wesel Germany). Impedance measurements were conducted using an SI 1255 H.F Frequency Response Analyzer (MESTEC GmbH, Munich).

2.3. Preparation of Anthracene Solution

0.022 g of anthracene was dissolved in 25 mL of acetonitrile to make a 5-mM solution that was used for subsequent experiments.

2.4. Preparation of the Modified Electrode

The GCE was cleaned by polishing with the alumina slurries in decreasing sizes of 1.0, 0.3, and 0.05 µm on polishing pads with thorough cleaning using water after each step. The polished GCE was put through ultrasonication in ethanol and subsequently in water for 5 min each before it was left to dry at room temperature. Then, 1 mg of MWCNTs was dispersed in 1 mL of DMF through ultrasonication for 1 hr. Afterwards, 5 µL of the dispersed MWCNTs were drop-coated onto the clean GCE and dried in an oven at 35 °C for 1 hr, which resulted in MWCNTs/GCE.

2.5. Impedance Measurements of the GCE and MWCNTs/GCE

Impedance measurements for the bare GCE and MWCNTs/GCE were conducted using a solution containing 5 mM $K_3Fe(CN)_6$, 5 mM $K_4Fe(CN)_6 \cdot 3H_2O$ and 0.1 M KCl. The solution was purged with N_2 for 5 min before the experiment. A frequency range of 1 Hz – 100 KHz was used, and the resulting data were fitted to equivalent circuits using Boukamp software (version 2.4).

2.6. Electrochemical Oxidation of Anthracene on GCE and MWCNTs/GCE

First, 0.1 M $LiClO_4$ in acetonitrile/water (80:20), as used by Tovide et al [13], was used as the supporting electrolyte solution. Anthracene was added to the supporting electrolyte solution to make 167 µM. The resulting solution was purged with N_2 for 5 min before analysis. Cyclic voltammetry was conducted in the potential range from −0.6 to +1.4 V with the scan rate of 50 $mV \cdot s^{-1}$ at the GCE and MWCNTs/GCE.

Variable concentrations of anthracene were analyzed at MWCNTs/GCE by adding 0.1-mL aliquots of a 5-mM anthracene solution to a 30-mL solution of the supporting electrolyte 0.1 M $LiClO_4$, which was N_2-purged for 5 min at the beginning of the experiment. Each addition was followed by stirring the solution for 5 min and 5 min of stillness to satisfy a 10-min accumulation time, which was determined to be necessary in the experiments. Cyclic voltammetry (CV) and square wave voltammetry were used in the analysis. The potential range and scan rate for CV were −0.6 to +1.4 V and 50 $mV \cdot s^{-1}$,

respectively. The parameters for square wave voltammetry were as follows: potential range, 0.7–1.4 V; pulse amplitude, 20 mV; frequency, 5 Hz; E_{step}, 10 mV; current range, 1 mA.

3. RESULTS AND DISCUSSION

3.1. Impedance Measurement

The modification of the GCE with MWCNTs caused an increase in charge transfer resistance from 237 Ω to 7570 Ω. The probable reason is that the walls of the MWCNTs are the points of contact between the MWCNTs and the surface of the GCE. The sites responsible for electrochemical activity in CNTs are the edge-plane sites, which are present at their edges instead of the walls [17]. A possible piling of the MWCNTs on the surface of the GCE would reduce the conductivity.

The Nyquist plot for the bare GCE is characterized by a semicircular part, which represents the charge transfer resistance, R_{ct}, and a linear part, which represents Warburg diffusion resistance, Z_{diff}, in the equivalent circuit used to fit the data (Fig. 1). R_{sol} is the solution resistance; Q and Y_0 are the constant phase element and admittance, respectively (Table 1).

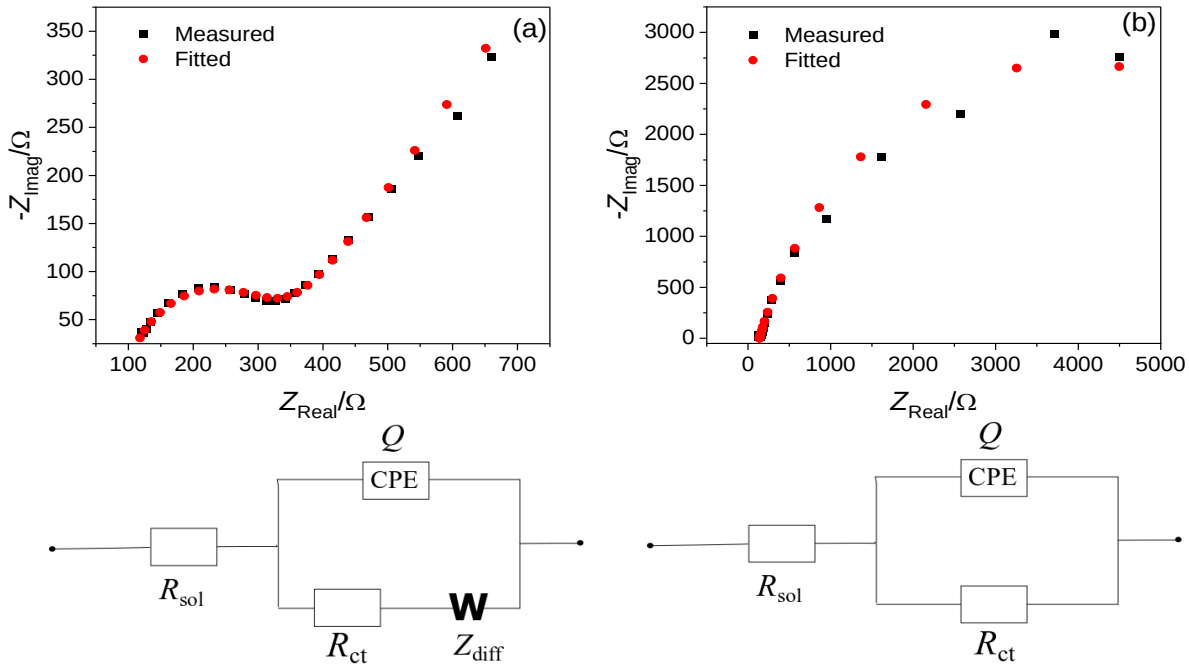

Figure 1. Nyquist plots for bare GCE (a) and MWCNTs/GCE (b) for impedance measurements in a solution containing 5 mM $K_3Fe(CN)_6$, 5 mM $K_4Fe(CN)_6 \cdot 3H_2O$ and 0.1 M KCl. Below the plots are the equivalent circuits used to fit their impedance data.

Table 1. Impedance data for bare GCE and MWCNTs/GCE

	R_{sol}/Ω	R_{ct}/Ω	Y_0 (= 1/Q)/S	Y_0 (= 1/Z_{diff})/10^{-4}S
GCE	97.8	2.37×10^2	9.35×10^{-6}	8.52
MWCNTs/GCE	139	7.57×10^3	6.59×10^{-4}	-

3.2. Electrochemical Oxidation of Anthracene

The electrochemical oxidation of anthracene at the bare GCE and MWCNTs/GCE was characterized by an oxidation peak with no reduction peak (Fig. 2). Thus, the electrochemical process was irreversible, which indicates the formation of stable products [18]. The proposed mechanism for the oxidation of anthracene based on ^{1}H NMR data includes the intermediates 9-anthranol, 9-anthrone, and 9,10-dihydroxyanthracene (Scheme 1). The products were 9,10-anthraquinone and bianthrone; the formation of the former is favored over the latter, especially in the presence of some water in acetonitrile [19]. The formation of 9,10-anthraquinone in the electrochemical oxidation of anthracene was further supported by spectroelectrochemical studies using surface enhanced Raman spectroscopy (SERS) [20]. The peak potential of the oxidation peak shifted by 53 mV to a less positive value at the MWCNTs/GCE, and the peak current was enhanced by 73.64%, which demonstrated the electrocatalytic activity of the modified electrode.

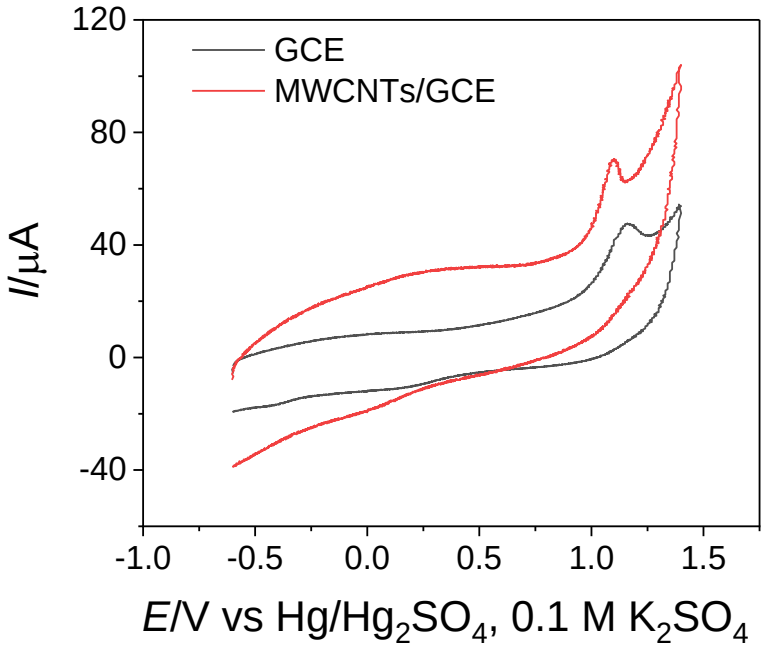

Figure 2. CVs of 167 μM anthracene in 0.1 M $LiClO_4$ GCE and MWCNTs/GCE at the scan rate of 50 $mV \cdot s^{-1}$

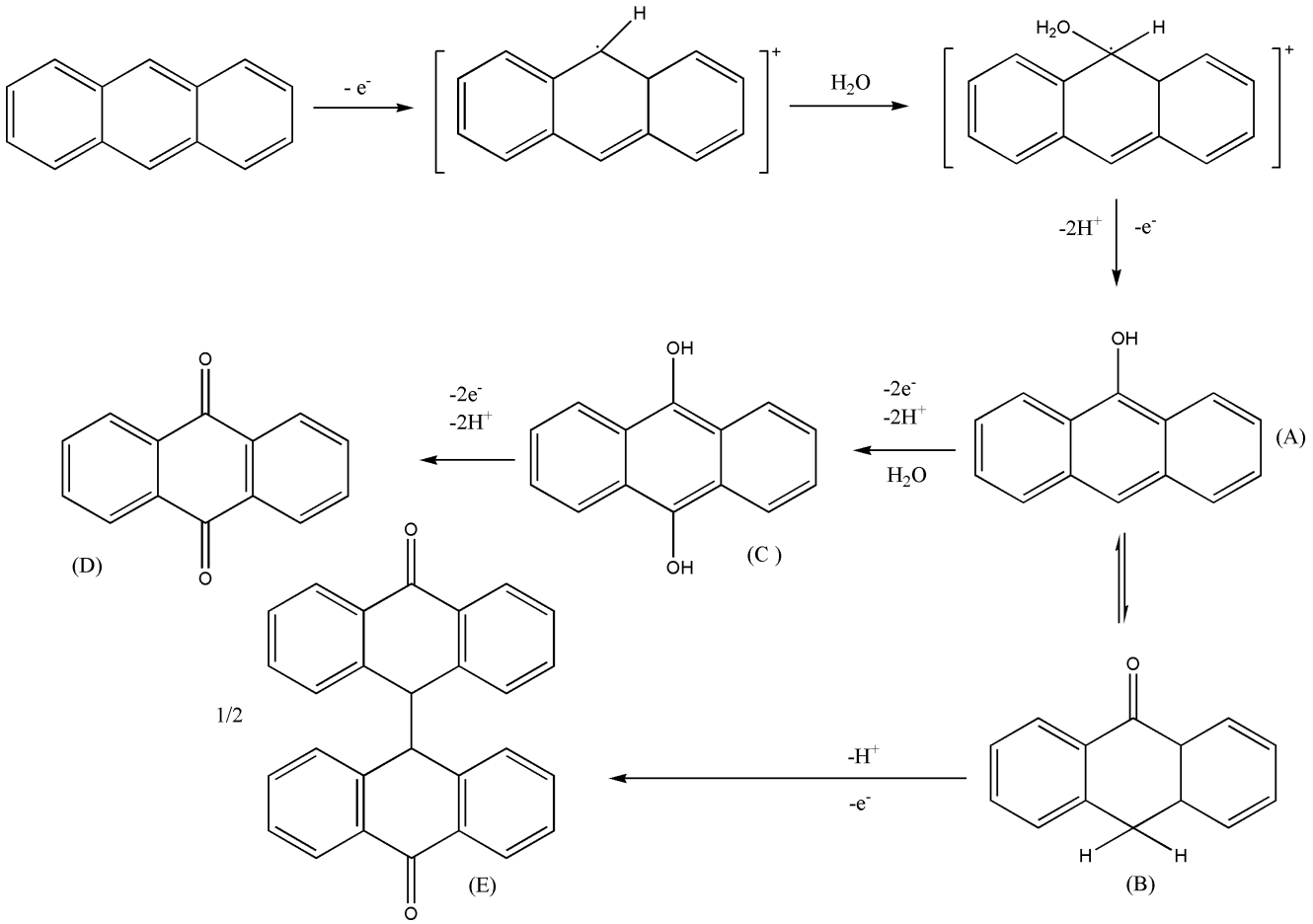

Scheme 1. A proposed mechanism for the electrochemical oxidation of anthracene, which shows the oxidation products 9-anthranol (A), 9-anthrone (B), 9,10-dihydroxyanthracene (C), anthraquinone (D), and bianthrone (E) [19].

Increase in scan rate was accompanied by a corresponding linear increase in peak current at the MWCNTs/GCE at scan rates of 50–175 mV·s^{-1} (Fig. 3a) The linear relationship described by I_{pa} = 0.32829v + 25.03952 with R^2 = 0.99498 is characteristic of adsorption-controlled electrochemical processes (Fig. 3b) [21]. I_{pa} and $v^{1/2}$ also had a linear relationship, which indicates a diffusion-controlled process (Fig. 3c). This result shows the mixed diffusion and adsorption control of the process. A plot of log I_{pa} vs. log v was linear with a slope of 0.55, which is between 0.5 and 1, the ideal values for diffusion-controlled and adsorption-controlled processes (Fig. 3d) [22].

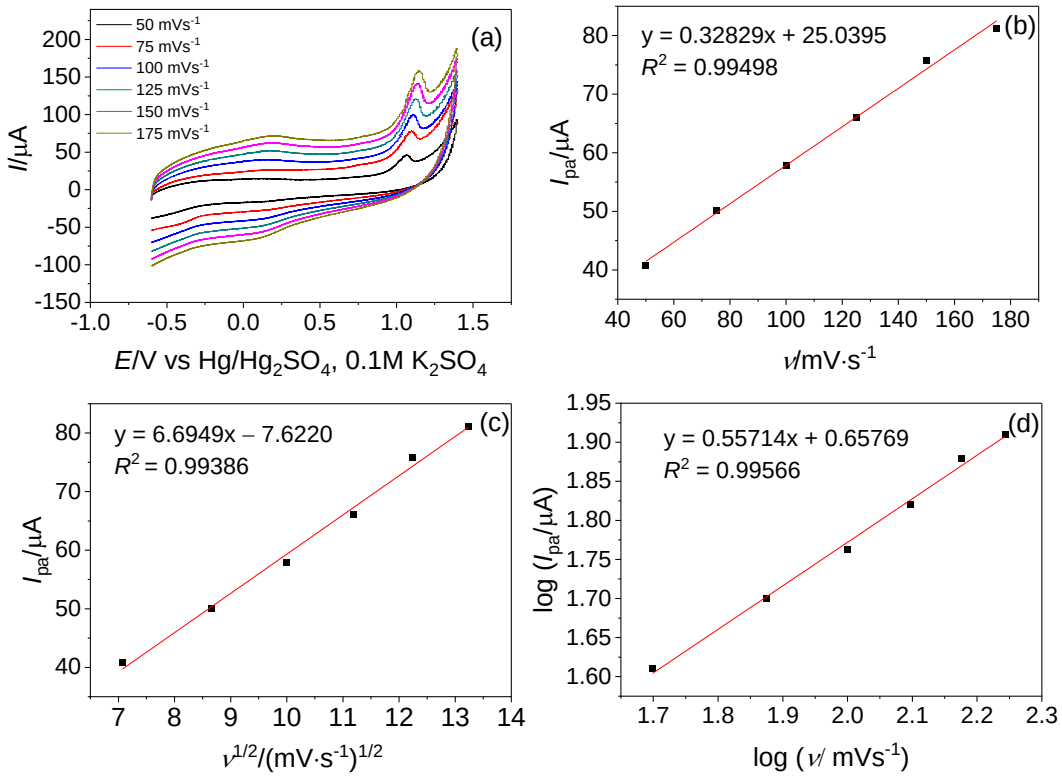

Figure 3. Cyclic voltammograms of MWCNTs/GCE in a solution of 167 µM anthracene and 0.1 M $LiClO_4$ at scan rates 50–175 $mV \cdot s^{-1}$ (a) and the corresponding plot of I_{pa} against v (b). Plot of I_{pa} against $v^{1/2}$ (c) and a plot of log v against log I_{pa} (d).

3.3. Effect of the Accumulation Time

Evidence of some effect of adsorption in the scan rate studies made it necessary to study the effect of the employment of a preconcentration or accumulation time in the analysis of anthracene. This was the time before a voltammetric measurement was made. It was observed that an increase in accumulation time caused an increase in peak current for anthracene oxidation (Fig. 4a) until 10 min of accumulation time, beyond which there was a reduction in peak current (Fig. 4b). The increase in peak current is probably a result of the adsorption of more analyte molecules on the modified surface with longer accumulation time.

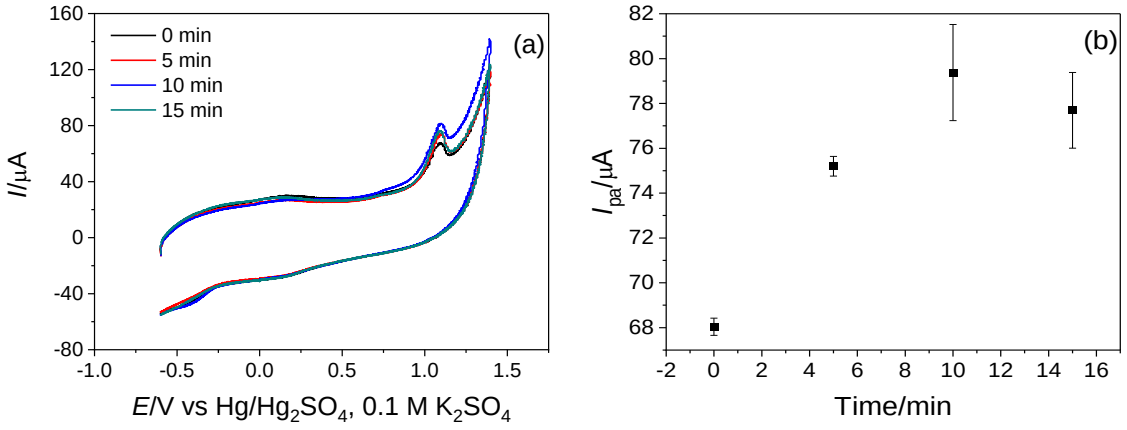

Figure 4. CVs of MWCNTs/GCE in a solution containing 167 μM anthracene and 0.1 M $LiClO_4$ at 50 $mV \cdot s^{-1}$ and different accumulation times (a) and a plot of I_{pa} versus accumulation time (b).

3.4. Voltammetric Analysis of Varying Concentrations of Anthracene

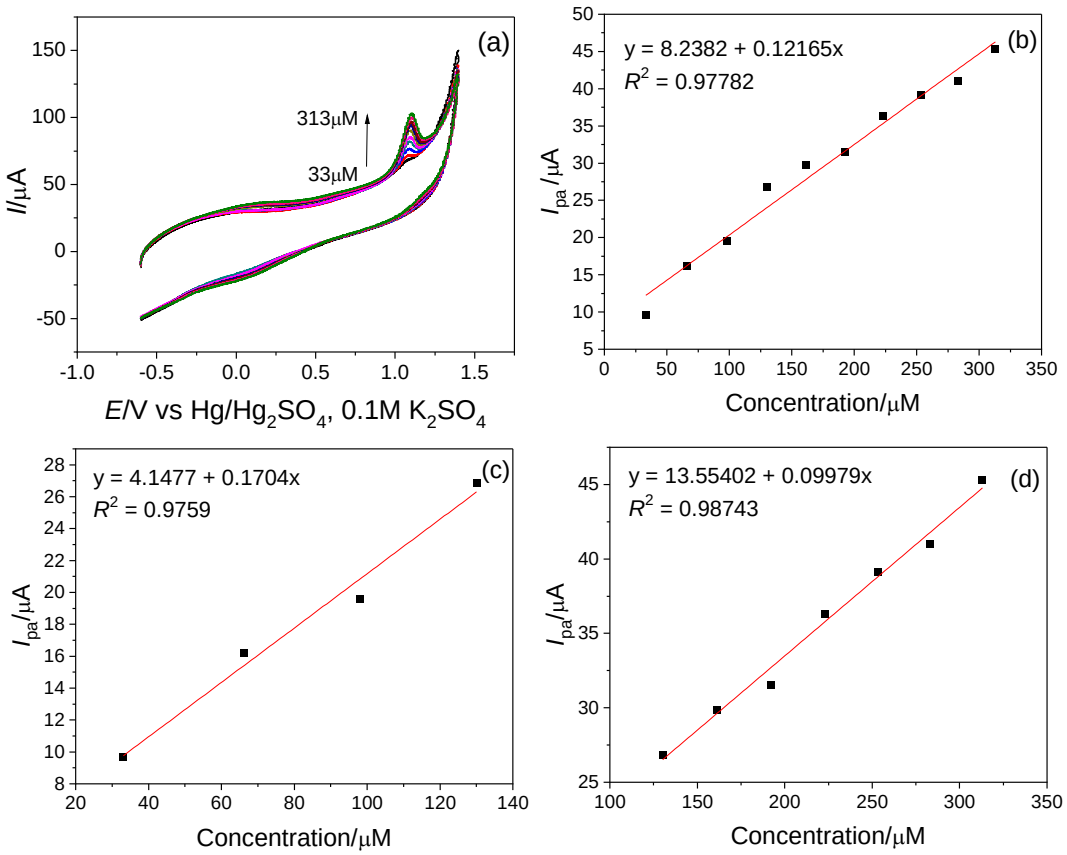

Figure 5. CVs of MWCNTs/GCE in increasing concentrations of anthracene (33–313 μM) in 0.1 M $LiClO_4$ at 50 $mV \cdot s^{-1}$ (a), and a plot of I_{pa} versus anthracene concentration (b). Plots of I_{pa} versus anthracene concentration in the dynamic ranges of 33–130 μM (c), and 130–313 μM (d).

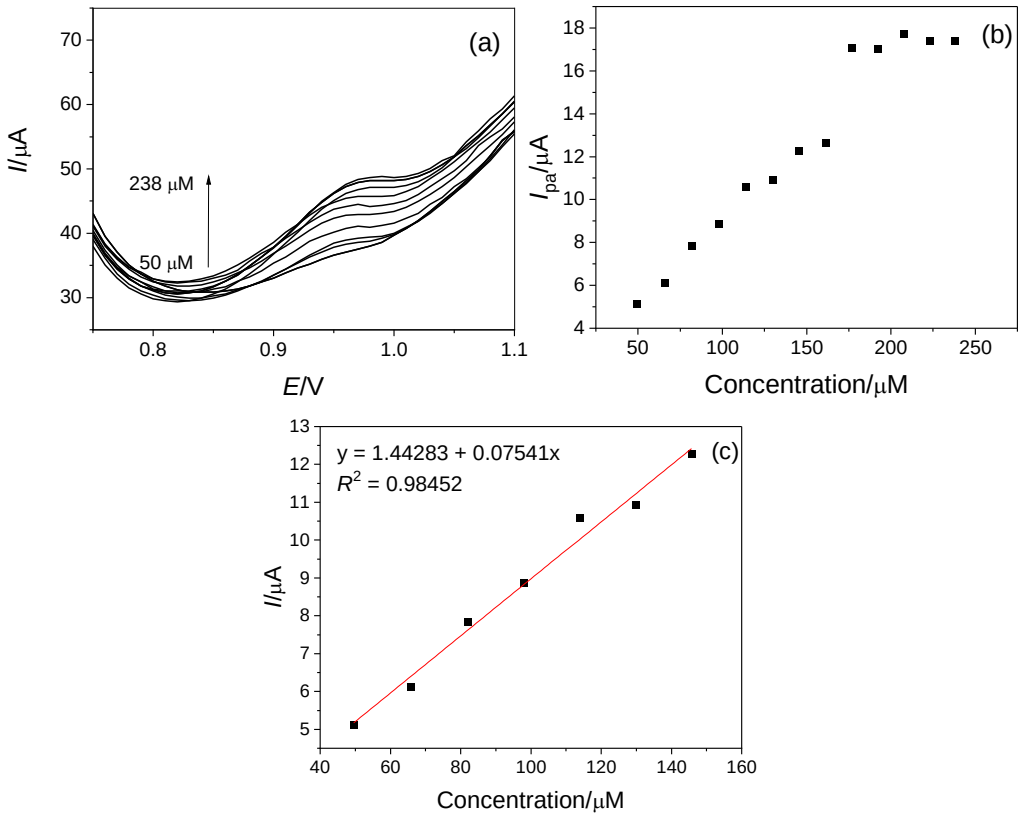

Figure 6. Square wave voltammograms of MWCNTs/GCE in increasing concentrations of anthracene in 0.1 M $LiClO_4$ (a). Plot of I_{pa} versus the concentration of anthracene (b) and the dynamic range of 49.5–145.63 µM (c).

Increasing concentrations of anthracene were analyzed using cyclic voltammetry and square wave voltammetry at MWCNTs/GCE. In cyclic voltammetry, an increase in peak current with the increase in concentration of anthracene was observed (Fig. 5a). When the peak current was plotted against the concentration of anthracene in the range of 33–313 µM, a linear relationship described by I_{pa} = 8.2382 + 0.12165*c* (*c* = concentration) and R^2 = 0.97782 was established (Fig. 5b). The limit of detection (LOD) was determined using the following equation:

$$LOD = 3\sigma/m \text{ [23]}$$

where σ is the standard deviation of the intercept given by S.E × $\sqrt{N}$ (*N* is the number of samples analyzed, and S.E is the standard error of the intercept). The LOD for the dynamic range of 33–313 µM was established to be 94 µM. Two possible dynamic ranges were also identified: 33–130 µM and 130–313 µM with R^2 of 0.9759 and 0.98743, respectively. The dynamic range of 33–130 µM is described by I_{pa} = 4.1477 + 0.1704*c*, while the dynamic range of 130–313 µM is described by I_{pa} = 13.55402 + 0.09979*c* (Figs. 5c & d). The LODs for the dynamic ranges of 33–130 µM and 130–313 µM were 48 µM and 84 µM, respectively.

In the square wave voltammetric analysis of increasing concentrations of anthracene, an increase in peak current was also observed with the increasing concentration (Fig. 6a). The peak current increased

up to the concentration of 161 µM, beyond which a saturation region was observed, where the peak current remained constant (Fig. 6b). The saturation region indicates that all active sites on the modified electrode had been occupied [24]. A dynamic range of 50–146 µM described by the equation I_{pa} = 1.44283 + 0.07541*c* (R^2 = 0.98452) was established. The LOD was 42 µM, which was not as low as the one achieved in previous studies by other researchers (Table 2). For example, Mailu et al [11] achieved a much lower LOD and a wider dynamic range. The other platforms suffered from either the interference of the modifying layer with a higher background current, e.g., the Au/Dendron employed by Rassie et al [12], or a modifying layer that likely degrades at higher potentials required for the oxidation of other PAHs (e.g., the PANI used by Tovide et al. [13]). Since a platform should be developed with a real sample in mind, a sensor for anthracene should consider that it does not occur in isolation in a real sample but in a mixture of other PAHs. Therefore, the platform including PANI will encounter challenges. The Au/dendron platform had another drawback: it was not selective to either anthracene or phenanthrene and could not distinguish between them. The present study has the advantage of a nondegrading modifying layer and a clear oxidation peak for anthracene, which can be distinguished from other PAHs. Because the oxidation potential of anthracene is shifted to a lower potential at MWCNTs/GCE, one can enhance the selectivity towards it by separating the oxidation peak from those of other PAHs. The adsorptive nature of MWCNTs/GCE can also be used to improve the sensitivity of the platform if more MWCNTs can be deposited to the GCE to form a stable layer. In the present study, it was observed that using more material (more than 1 mg/1 mL) to make the MWCNTs dispersion in DMF resulted in an unstable layer that easily peeled off. Work is currently underway to find a solution to that problem.

Table 2. Analytical parameters obtained in previous studies on electrochemical detection of anthracene

Platform	LOD/µM	Dynamic range/µM	Reference
PPyox/Ag-AuNPs/GCE	0.169	3.0 – 356	[11]
Au/Dendron	Not reported	Not reported	[12]
GR-PANI/GCE	0.0044	0.012 – 1000	[13]
MWCNTs/GCE	42	50 – 146 µM	Present work

PPyox – Overoxidized polypyrrole, GR – Graphene, PANI - Polyaniline

3.4. Determination of Anthracene in Tap Water

Detection of anthracene in tap water using MWCNTs/GCE was also attempted. A portion of the spiked tap water was mixed with acetonitrile in the ratio of 1:4 to reach a concentration that fit in the square wave voltammetry dynamic range. $LiClO_4$ was added to the mixture to make a concentration of 0.1 M. Since the initial amount of anthracene spiked into the tap water from a 5-mM solution of anthracene was high, some of it precipitated out of the solution because of its low solubility in water (0.075 mg/L at 25 °C [25]). This precipitation of anthracene out of the solution resulted in much lower concentrations of anthracene than expected being detected in the final solution, and this concentration decreased with the increase in initial concentration (Table 2). However, this procedure of

electrochemical detection of anthracene can be more effective when used with a more sensitive platform, which implies that a lower initial concentration spiked into tap water will reduce all losses due to precipitation.

Table 3. Percentage of the amount of anthracene detected in spiked tap water

Amount Expected/μM	Average I_{pa}/μA	Standard deviation (n = 3)	Amount detected/μM	% Detected
60	4.983	0.103	47	78
100	5.583	0.101	55	55

4. CONCLUSIONS

A modification of the GCE with MWCNTs appeared to reduce the conductivity of the modified electrode, but it resulted in an enhanced peak current and a shift of the peak potential to a less positive value for the anthracene oxidation. The electrochemical oxidation of anthracene on the modified electrode was mixed diffusion- and adsorption-controlled, and the effect of adsorption necessitated the use of preconcentration or accumulation time in the analysis of anthracene. The lowest limit of detection in the electrochemical detection of anthracene on the modified electrode was 42 μM, and the dynamic range was 50–146 μM. Although the limit of detection was not as low as those in previous efforts, the electrochemical behavior of anthracene on the modified electrode can be used in future development of an electrochemical sensor for anthracene. In the electrochemical detection of anthracene introduced in tap water, lower concentrations than expected were detected because of the low solubility of anthracene in water, resulting in some of it precipitating out of the solution on addition to tap water. However, the procedure can be applied to more sensitive detection platforms.

ACKNOWLEDGEMENTS
Funding for this work was provided by the Deutscher Akademischer Austauchdienst (DAAD).

References

1. Agency for Toxic Substances and Disease Registry, *Toxicological profile for polycyclic aromatic hydrocarbons*, Ed. M. Mumtaz and J. George, US Department of Health and Human Services, Public Health Service, (1995) Atlanta Georgia, US (accessed Oct. 23, 2019) https://www.atsdr.cdc.gov/toxprofiles/tp69.pdf.
2. Z. Zelinkova and T. Wenzl, *Polycyclic. Aromat. Compd.*, 35 (2015) 248.
3. IARC, Ed., *Polynuclear aromatic compounds Pt. 1: Chemical, environmental and experimental data*, vol. 32. International Agency for Research on Cancer (1983) Lyon, France.
4. World Health Organization, Ed., *Air quality guidelines for Europe*, 2nd ed. World Health Organization (2000) Regional Office for Europe, Copenhagen, Denmark.
5. N. T. Edwards, *J. Env. Qual.*, 12 (1983) 427.
6. Office of the US EPA, *Safe Drinking Water Act* (SDWA), *US EPA*, 2015. https://www.epa.gov/sdwa (accessed Oct. 22, 2019).

7. Official Journal of the European Communities, *Directive 2013/39/EU of the European Parliament and of the Council of 12 August 2013 amending Directives 2000/60/EC and 2008/105/EC as regards priority substances in the field of water policy text with EEA relevance*. p. 17.
8. A. H. Colmsjo, *The Handbook of Environmental Chemistry Part 1: PAHs and Related Compounds*. Springer-Verlag (1998) New York, US.
9. R. Ferrer, J. Guiteras, and J. L. Beltran, *J. Chromatogr. A*, 779 (1997) 123.
10. A. E. Eiroa, M. P. Lopez, L. S. Muniategni, R. D. Prada, and F. E. Fernandez, *Talanta*, 51 (2000) 677.
11. S. N. Mailu, T. T. Waryo, P. M. Ndangili, R. N. Fanelwa, A. A. Balag, P. G. Baker, and E. I. Iwuoha, *Sensors*, 10 (2010) 9449
12. C. Rassie, R. A. Olowu, T. T. Waryo, L. Wilson, A. Williams, P. G. Baker, and E. I. Iwuoha, *Int. J. Electrochem. Sci.*, 6 (2011) 19.
13. O. Tovide, N. Jahed, C. E. Sunday, K. Pokpas, R. F. Ajayi, H. R. Makelane, K. M. Molapo, S. V. John, P. G. Baker, and E. I. Iwuoha, *Sens. Actuators, B*, 205 (2014) 184.
14. C. E. Banks, A. Crossley, C. Salter, S. J. Wilkins, and R. G. Compton, *Angew. Chem. Int. Ed.*, 45 (2006) 2533.
15. R. H. O. Montes, J. S. Stefano, E. M. Richter, and R. A. A. Munoz, *Electroanalysis*, 26 (2014) 1449.
16. D. Boikanyo, *Electrochemical Study of Pyrene Using Glassy Carbon Electrode Modified with Metal-Oxide Nanoparticles and a Graphene Oxide / Multi- Walled Carbon Nanotubes Nanoplatform*, Master of Science Thesis (2015), North-West University, South Africa.
17. C. E. Banks, T. J. Davies, G. G. Wildgoose, and R. G. Compton, *Chem. Commun.*, 7 (2005) 829.
18. D. A. C. Brownson and C. E. Banks, Interpreting Electrochemistry in *The Handbook of Graphene Electrochemistry*, Springer London (2014) London, UK
19. C. A. Paddon, C. E. Banks, I. G. Davies, R. G. Compton, *Ultrason. Sonochem.*, 13 (2006) 126
20. D. S. Cordeiro and P. Corio, *J. Braz. Chem. Soc*. 1 (2009) 80.
21. N. Elgrishi, K. J. Rountree, B. D. McCarthy, E. S. Rountree, T. T. Eisenhart, and J. L. Dempsey, *J. Chem. Educ.*, 95 (2018) 197.
22. A. J. Bard and L. R. Faulkner, *Electrochemical methods: fundamentals and applications*, 2nd ed. Wiley (2001) New York, US.
23. H. Hrichi, M. R. Louhaichi, L. Monser, and N. Adhoum, *Sens. Actuators, B*, 204 (2014) 42.
24. J. Janata, *Principles of Chemical Sensors*, Second Ed. Springer (2009) Dordrecht, Heidelberg, London, New York.
25. M. M. Miller, S. P. Wasik, G. Lan. Huang, W. Ying. Shiu, and Donald. Mackay, *Environ. Sci. Technol.*, 19 (1985) 522.